# DESIGN OF A HIGH VOLTAGE RESONANCE PULSER

**S.H. Nam[ξ], S.S. Park, H. Heo, S.C. Kim, S.H. Kim, J.W. Shin[†] , J.H. So[†] , and W. Jang[†]**
*Pohang Accelerator Laboratory, Pohang, 790-784 Korea*
[†] *ADD, Daejeon, 305-102 Korea*

## *Abstract*

It is beneficial to use a resonant pulse transformer charging circuit for designing of a high voltage generator. A high voltage triple resonant generator is designed. A high voltage air core transformer is used in the circuit. Triple resonant charging circuit with the transformer is used to step up the primary voltage. The voltage step-up ratio is designed as about eleven at the charging stage. A distributed pulse forming network (PFN) is used to form a square output waveform. The output has an over-volted spark-gap switch that transfers energy to a matched resistive load with a distributed PFN. The generator is positioned in a cylindrical transformer oil tank. Height and diameter of the tank are respectively 1.06 m and 1.28 m. A dummy water load and a beam stick are used to test the generator. Design procedures and preliminary test results are discussed.

## I. TRIPLE RESONANCE CHARGING PULSE TRANSFORMER CIRCUIT

A triple resonance charging pulse transformer circuit is designed [1, 2]. An air core step-up pulse transformer is employed in the circuit [3, 4]. Load impedance of about 100 ohm was our initial goal for the design. The desired output pulse width and voltage are respectively around 200 ns and 200~500 kV. A base design condition was to use four 60 nF/100 kV capacitors, which was in stock in our lab. Triple resonant circuit has more flexibility than the double resonant circuit to design with a given primary capacitance and a load impedance. Moreover, using the triple resonance, we can substantially reduce high voltage stress across the pulse transformer. This is a very important feature in high voltage generators since the pulse transformer is one of the troublesome components in the generators due to breakdown by the voltage stress. Fig. 1 shows the basic circuit diagram of the system. Fig. 2 represents a schematic of the triple resonant charging circuit. An equivalent circuit of the Fig. 2, seen at the primary side, is shown in Fig. 3. The circuit has a purely oscillatory transient response with three natural frequencies $\omega_1$, $\omega_2$, and $\omega_3$. At the resonant condition of the circuit in Fig.2, 100% of the energy initially stored in the capacitor $C_1$ is transferred to the capacitor $C_3$. This occurs when the three normal mode frequencies $\omega_1=k\,\omega_0$, $\omega_2= l\omega_0$, and $\omega_3=m\omega_0$ are in the ratio of whole numbers $k$, $l$, and $m$ where $l=k+1, k+3, k+5, \ldots$ and $m=l+1, l+3, l+5, \ldots$ . The most commonly used two simplest resonant modes are formed when the ratio of $\omega_1 : \omega_2 : \omega_3$ are 1:2:3 and 1:2:5. In the table 1, the triple resonant conditions on circuit components are given for the ratio 1:2:3 and 1:2:5.

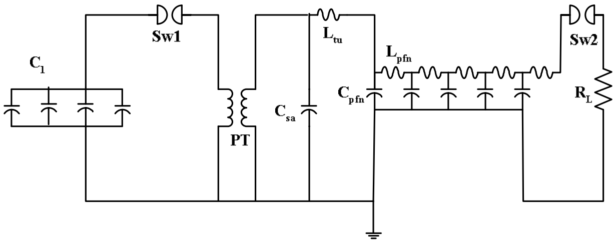

**Figure 1.** Conceptual circuit diagram of the triple resonant charging and self discharging system. $C_1$=Capacitor Bank, Sw1= Triggered Primary Charging Switch, PT=Pulse Transformer, $C_{sa}$=Secondary Auxiliary Capacitor, $L_{tu}$= Tuning Inductor, $L_{pfn}$= Distributed PFN Inductor, $C_{pfn}$ (or C3)= Distributed PFN Peaking Capacitor, Sw2= Over-Volted Output Switch, $R_L$= Load.

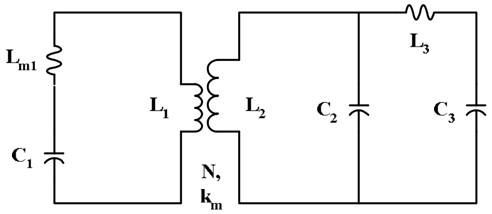

**Figure 2.** A schematic of the resonant circuit. $L_{m1}$=Pri. stray inductance. $L_1$=Pri. inductance of the transformer, $L_2$= Sec. inductance of the transformer, N=Transformer turn ratio, $k_m$= Transformer coupling coefficient, $C_2 = C_{sa}+C_{PT}$ (where, $C_{PT}$ = transformer stray capacitance), $L_3= L_{tu}+L_{pfn}$ = Tuning inductance. Resistive components are ignored.

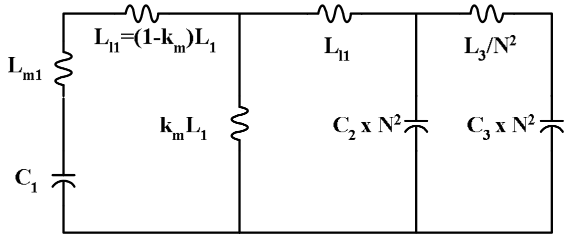

**Figure 3.** Equivalent circuit of the circuit shown in Fig. 2. $L_{11}=(1-k_m)L_1$=Leakage inductance of the transformer.

---

[ξ] email: nsh@postech.ac.kr

1-4244-0914-4/07/$25.00 ©2007 IEEE.

**Table 1.** Triple Resonance Circuit Parameters

| | $k:l:m=$ 1:2:3 | Criteria | $k:l:m=$ 1:2:5 |
|---|---|---|---|
| $\omega_0^2 L_1 C_1$ | $\frac{11}{24}$ | $\frac{2m^2k^2+(m^2-l^2)(l^2)(l^2-k^2)}{2k^2l^2m^2}$ | $\frac{113}{200}$ |
| $\omega_0^2 L_2 C_2$ | $\frac{4}{9}$ | $\frac{l^2}{k^2m^2}$ | $\frac{4}{25}$ |
| $\omega_0^2 L_3 C_3$ | $\frac{1}{4}$ | $\frac{1}{l^2}$ | $\frac{1}{4}$ |
| $k_m^2$ | $\frac{5}{11}$ | $\frac{(m^2-l^2)(l^2-k^2)}{2k^2m^2+(m^2-l^2)(l^2-k^2)}$ | $\frac{63}{113}$ |
| $\frac{L_2}{L_3}$ | $\frac{5}{6}$ | | $\frac{63}{50}$ |

**Table 2.** Calculated component values with the 1:2:3 ratio.

| **Parameter** | **Symbol** | **Cal.** | **Unit** |
|---|---|---|---|
| Pri. Ind. | $L_1$ | 773.9 | nH |
| Sec. Ind. | $L_2$ | 84.4 | µH |
| Tuning Ind. | $L_3$ | 101.3 | µH |
| Main Cap. | $C_1$ | 240 | nF |
| Sec. Cap. | $C_2$ | 2133.3 | pF |
| Peaking Cap. | $C_3$ | 1000 | pF |
| Turn Ratio | N | 10.4 | |
| Coupling Coefficient | $k_m$ | 0.67 | |
| Leakage Inductance | $L_{l1}$ | 252.2 | nH |

**Table 3.** Air Core Pulse Transformer Design Parameters

| **Parameter** | **Symbol** | **Value** | **Unit** |
|---|---|---|---|
| Primary Inductance | $L_1$ | 786.56 | nH |
| Primary Resistance | $R_p$ | <100 | mΩ |
| Secondary Inductance | $L_2$ | 83.91 | µH |
| Primary Number of Turn | $N_p$ | 1 | |
| Secondary Number of Turn | $N_s$ | 11 | |
| Secondary Resistance | $R_s$ | 33.914 | mΩ |
| Coupling Coefficient | $k_m$ | 0.6742 | |
| Secondary Capacitance | $C_s$ | 586 | pF |
| Core | Air | | |
| Type | Isolation | | |

In Table 2, calculated component values of the ratio 1:2:3 are given. Initial fixed values for the calculation are $C_1$, $C_3$, and $f_0$, which are respectively 240 nF, 1nF, and 250 kHz. For the calculation, $L_{ml}$ is ignored. Based on the calculation in Table 2, design parameters of the air core transformer are calculated and listed in Table 3 [5, 6, 7]. In Table 4, design values of other components, excluding the pulse transformer,  are listed. There exist some discrepancy between the calculated values in Table 2 and the design parameters in Table 4. This happens during design procedures to adopt real physical dimensions of the components.

**Table 4.** Design Parameters of Various Components in the Triple Resonant Circuit.

| **Parameter** | **Symbol** | **Value** | **Unit** |
|---|---|---|---|
| Total Pri. Stray Ind. | $L_{ml}$ | <200 | nH |
| Total Sec. Cap. | $C_2$ | 2133 | pF |
| Sec. Cap. | $C_{sa}=C_2-C_s$ | 1547.75 | pF |
| Tuning Inductor | $L_{tu}$ | 97.66 | µH |
| Total PFN Cap. | $C_{pfn}$ or $C_3$ | 1051.3 | pF |
| Total PFN Ind. | $L_{pfn}$ | 10.44 | µH |
| Total Sec. Ind. | $L_3=L_{tu}+L_{pfn}$ | 108.09 | Mh |

## II. CIRCUIT SIMULATION

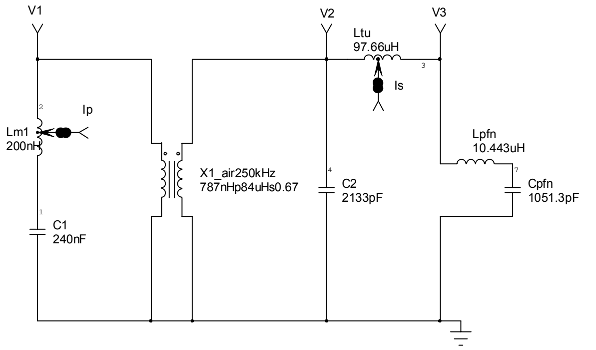

**Figure 4.** Pspice simulation circuit.

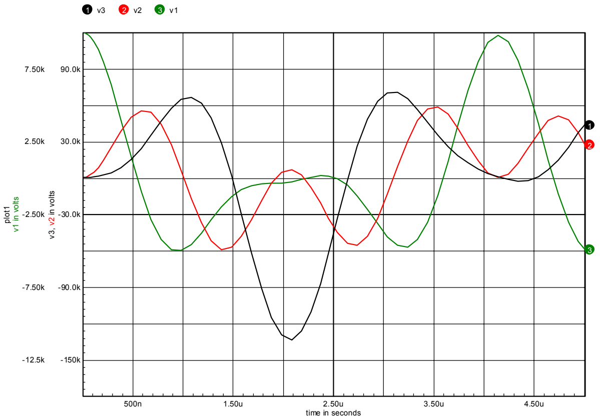

**Figure 5.** Simulation result of the triple resonance charging (10 kV charging, $L_{m1}$=1 nH, 1st peak of $V_2$ = 55 kV, Maximum peak of $V_3$= -133.8 kV). 500 ns/Div., V1: Transformer primary voltage (2.5 kV/Div.), V2: Transformer secondary voltage (30 kV/Div.), V3: Final charging voltage (30 kV/Div.).

By using the design parameters, the Pspice circuit simulation is performed. The simulation circuit is shown in Fig. 4. Since the primary stray inductance, $L_{m1}$, is not known, it is selected as a variable to find allowable range, at which the resonance condition is maintained in an acceptable level. Fig. 5 shows a simulation result when the $L_{m1}$ is 1 nH. As shown, when the final charging voltage is maximum at 2.1 µs, the primary and secondary voltage amplitude of the pulse transformer is almost zero. Therefore, the resonant condition is well satisfied, implying that all energy is transferred to the PFN capacitor. $L_{m1}$ values are increased up to 200 nH, which is practically realizable value in fabrication, and find that no significant resonant waveform distortion is found.

## III. PFN OUTPUT CIRCUIT

When the charging voltage reaches to the peak, self-breakdown of the final spark gap switch in Fig. 1 is induced to transfer square shaped energy to the load. To form the square shape output waveform, distributed PFN is used. Design parameters of the PFN is given in Table 5.

**Table 5.** Parameters of the PFN output circuit

| **Parameter** | **Symbol** | **Value** | **Unit** |
|---|---|---|---|
| Total PFN Capacitance | $C_{pfn}$ | 1051.3 | pF |
| Total PFN Inductance | $L_{pfn}$ | 10.44 | µH |
| PFN Impedance | $Z_{pfn}$ | 99.67 | Ω |
| Load (RKA) Impedance | $R_L$ | 100 | Ω |
| Output Pulse Width | $T_w$ | 210 | ns |

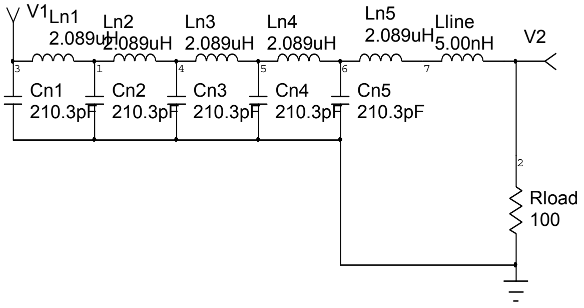

**Figure 6.** Spice simulation circuit of the pulse forming (or peaking) and the output section of the triple resonance circuit.

The output circuit is also simulated by assuming a five section passive type-E PFN, and the circuit is shown in Fig. 6. The simulation result is shown in Fig. 7. It is assumed impedance matching between the PFN and the load, and therefore the output voltage is a half of the charging voltage peak. Pulse width follows well the design parameter.

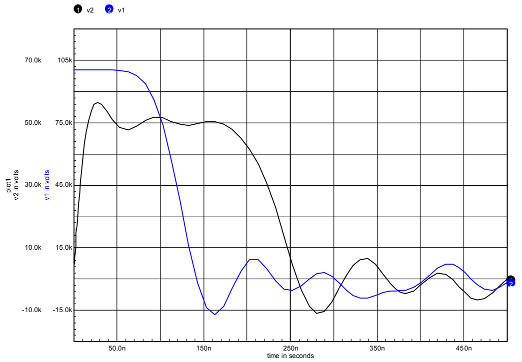

**Figure 7.** Spice simulation result from the output circuit with 100 kV PFN charging.

## IV. FABRICATION OF CIRCUIT COMPONENTS

### A. Air Core Pulse Transformer Design

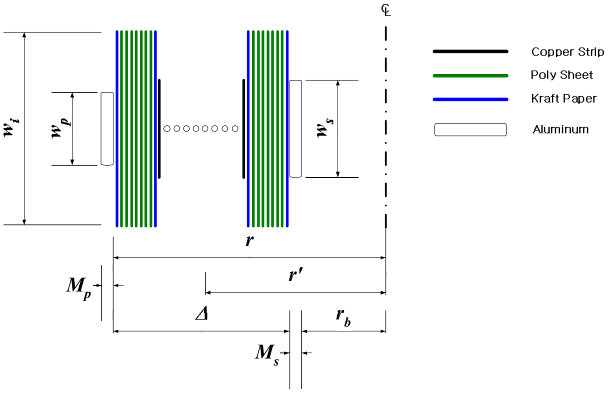

**Figure 8.** Conceptual drawing of the air core spiral strip pulse transformer.

**Table 6.** Physical dimensions of the pulse transformer

| Parameter | Symbol | Value | Unit |
|---|---|---|---|
| Outer Winding Radius | $r$ | 24.317 | Cm |
| Mean Winding Radius | $r'$ | 23.909 | Cm |
| Cylindrical Bobbin Radius | $r_b$ | 22.5 | Cm |
| Primary Strip Winding Thickness | $M_p$ | 10 | Mm |
| Final Turn Secondary Winding Thickness | $M_s$ | 10 | Mm |
| Secondary Strip Winding Thickness | $m_w$ | 0.007 | Cm |
| Number of Primary Turn | $N_p$ | 1 | |
| Number of Secondary Turn | $N_s$ | 11 | |
| Winding Thickness | $\Delta$ | 0.817 | cm |
| Primary Winding Width | $w_p$ | 9 | cm |
| Secondary Winding Width | $w_s$ | 12 | cm |
| Insulator Width | $w_i$ | 35 | cm |

The most important and difficult component to manufacture is the air core pulse transformer. In Fig. 8, conceptual fabrication drawing is presented. It is a spiral strip transformer. A cylindrical bobbin is used to wind the secondary winding strips and the primary aluminum strip [8]. The primary and the secondary windings are isolated. Detail physical dimensions of the transformer are listed in Table 6.

### *B. Other Components*

The secondary capacitance, $C_2$, is formed with the summation of the stray capacitance of the transformer, $C_s$, and the secondary auxiliary capacitance, $C_{sa}$. The $C_{sa}$ is fabricated as a parallel plate capacitor. The measured value was 1547.75 pF. The tuning inductor, $L_{tu}$, is made as an air core cylindrical inductor and the value is calculated using the following Wheeler's formula. Parameters of the tuning inductor are listed in Table 7.

Wheeler's Formula: $$L_{tu} = \frac{4 \times a_{tu}^{2} N_{tu}^{2}}{b_{tu} + 0.9 a_{tu}}.$$

**Table 7.** Parameters of the tuning inductor.

| Parameter | Symbol | Value | Unit |
|---|---|---|---|
| Number of Turns | $N_{tu}$ | 12.5 | |
| Coil Radius | $a_{tu}$ | 25 | cm |
| Coil Length | $b_{tu}$ | 17.5 | cm |
| Tuning Inductance | $L_{tu}$ | 97.66 | μH |

The overvolted output switch is a high pressure gas filled spark gap. Mixture of $SF_6$ and $N_2$ is used as the filling gas of the output switch.

### *C. Fabrication*

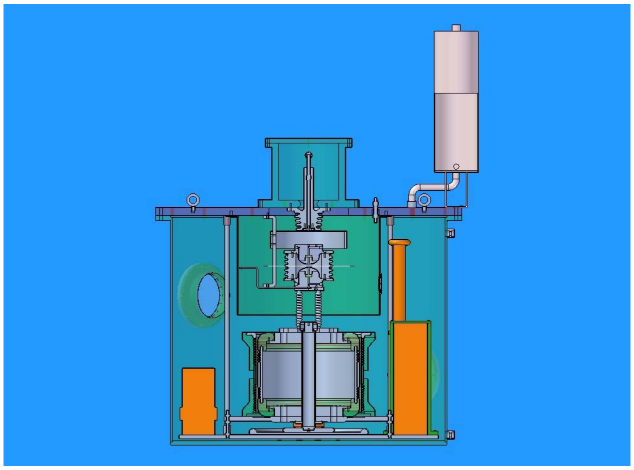

**Figure 9.** CAD drawing of the triple resonant system.

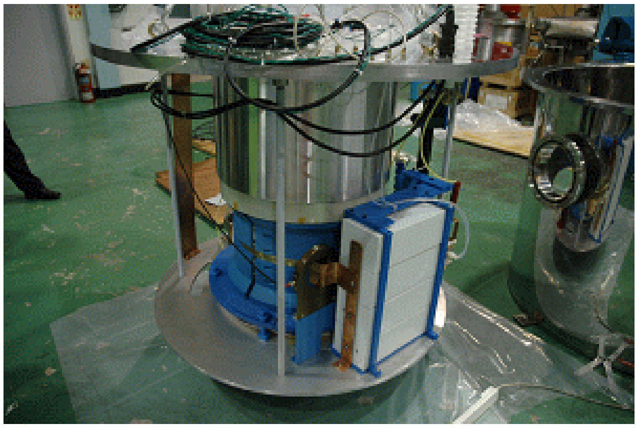

**Figure 10.** Assembled view of the triple resonant system.

In Fig. 9, a CAD drawing of the system is shown. The system is housed in a cylindrical stainless steel tank that is filled with transformer insulation oil. The tank dimensions are 1.28 m diameter, and 1.06m height. The pulse transformer is positioned at the lower center of the tank. A dummy water load is placed on top of the tank. In Fig. 10, a photo of the internal component assembly of the system is shown.

## V. PRELIMINARY TEST RESULT

Preliminary test of the system is performed, and the results are shown in Fig. 11 and 12. In Fig. 11, the charging voltage waveform of the PFN capacitor without the output switch breakdown is shown. Primary DC charging voltage was 11 kV and the final charging voltage peak is 126 kV. Therefore, the voltage step-up ratio is 11.5. As expected, the waveform follows well the simulated waveform.

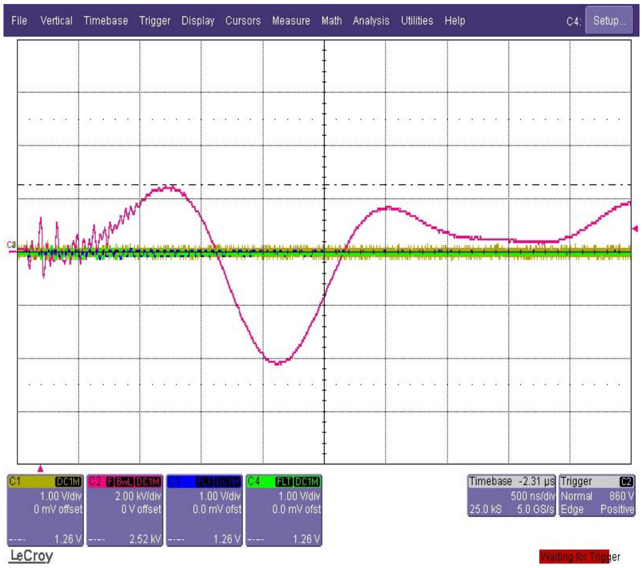

C1 DC1M 1.00 V/div 0 mV offset 1.26 V
C2 F BwL DC1M 2.00 kV/div 0 V offset 2.52 kV
C3 FLT DC1M 1.00 V/div 0.0 mV ofst 1.26 V
C4 FLT DC1M 1.00 V/div 0.0 mV ofst 1.26 V
Timebase -2.31 μs 500 ns/div 25.0 kS 5.0 GS/s
Trigger C2 Normal 860 V Edge Positive

**Figure 11.** The final resonant charging voltage waveform at 11 kV primary DC charging. The peak is 126 kV.

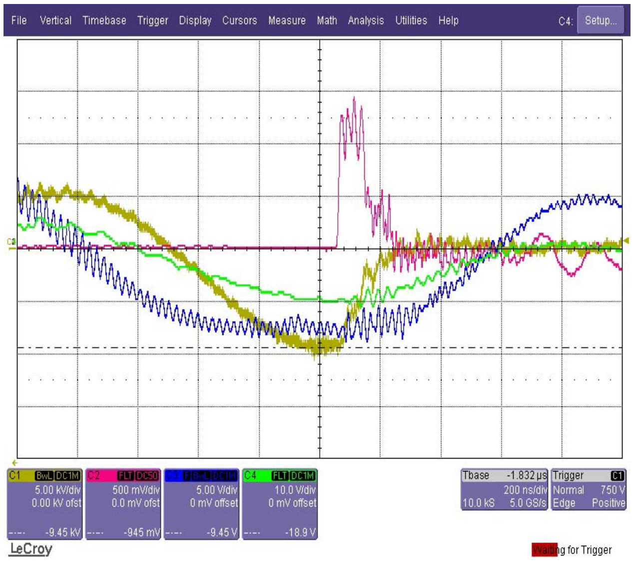

**Figure 12.** Resonant charging voltage and the output current waveforms of the system.

In Fig. 12, waveforms of the charging voltage as well as the output current are shown. At the peak of the charging, the output switch is breakdown in Fig. 12. Primary DC charging voltage (Ch4) was 21 kV. The secondary voltage peak (Ch3) is about 150 kV, and the final charging voltage peak (Ch1) is about 285 kV. The output switch was filled with $N_2$ gas at 2.1 kg/cm$^2$ pressure. The tested load impedance was 200 Ω, and the peak load current measured was 575 A. The pulse width of the output wave is narrower than the designed value. This occurs because the PFN component values actually manufactured was lower than the design value. The PFN component values will be fabricated again to reflect the original design parameters and the test will be resumed.

## VI. CONCLUSION

A triple resonant pulse transformer system is designed and manufactured. The expected output of the system is several hundred kV voltage output with about 200 ns pulse width in a 100 Ω load. The system is very compact in size (1.28 m diameter and 1.06 m height). An air cored spiral strip pulse transformer is also designed and manufactured. To reduce voltage stress on the pulse transformer, triple resonant circuit is used in the system. Total voltage step-up ratio is about 11. The desired output waveform is square. To form the square waveform, a distributed PFN is used. A high pressure overvolted spark gap switch is used to transfer the charged energy to the load. Preliminary test resembled the design values, except the pulse width. The peak output voltage tested was up to 300 kV.

## VII. REFERENCES

[1] F.M. Bieniosek, “Triple resonance pulse transformer circuit,” Rev. Sci. Instrum. 61(6), June 1990 pp1717-1719.

[2] F.M. Bieniosek, “Triple Resonance High Voltage Pulse Transformer Circuit,” 1987 the 6th IEEE Pulsed Power Conf. Proc., pp700-702.

[3] James P. O’Loughlin, “Air Core Pulse Transformer Design”, Power Modulator Conference 1988, pp325 – 330

[4] G. J. Rohwein, “A Low Impedance High-Voltage Direct Drive Transformer System”, 1988 IEEE Power Modulator Symposium proceeding, pp. 331 – 335

[5] Jing Luo, B.M. Novac, I.R. Smith, and J. Brown, “Fast and accurate two-dimensional modeling of high-current, high-voltage air-cored transformers,” J. Phys. D: Appl. Phys. 38(2005) 955-963.

[6] S. T. Ko, and S. H. Nam, “Numerical field analysis for an air cored spiral strip type pulse transformer”, 2004 Power Modulator Conference, May. 23-26, 2004, San francisco, CA, USA.

[7] S.T. Ko, S.H. Nam, “Field Enhancement Optimization of an Air-Cored Spiral Strip Pulse Transformer,” IEEE Tran. on Plasma Science, Vol. 33, No. 4, August 2005, pp 1268-1272.

[8] S.C. Kim, H. Heo, S.S. Park, S.H. Kim, S.H. Nam, "Development of an Air-Core Cylindrical HV Pulse Transformer," IEEE Int. Power Modulator Conf. 2006, Washington D.C., May 14-18, 2006.